Three-Dimensional Tomographic Features of Dome-Shaped Macula by Swept-Source Optical Coherence Tomography

ABDALLAH A. ELLABBAN, AKITAKA TSUJIKAWA, AKIKO MATSUMOTO, KENJI YAMASHIRO, AKIO OISHI, SOTARO OOTO, ISAO NAKATA, YUMIKO AKAGI-KURASHIGE, MASAHIRO MIYAKE, HUSSEIN S. ELNAHAS, TAREK M. RADWAN, KHALED A. ZAKY, AND NAGAHISA YOSHIMURA

• PURPOSE: To study the tomographic and pathomorphologic features of dome-shaped maculas with swept-source optical coherence tomography (OCT).

• DESIGN: Prospective, cross-sectional study.

• METHODS: The macular area of 51 highly myopic eyes (35 patients) with dome-shaped maculas was studied with swept-source OCT at 1050 nm. Three-dimensional (3-D) data sets were obtained with raster scanning covering a 12 × 8-mm^2 area; 3-D images of the posterior pole were constructed by autosegmentation of the retinal pigment epithelium (RPE).

• RESULTS: In all reconstructed 3-D images of the RPE, 2 outward concavities were seen within the posterior staphyloma and a horizontal ridge was formed between these 2 concavities. In 42 of these eyes, this horizontal ridge was band shaped. The vertical OCT section through the fovea showed a convex configuration of RPE, but the horizontal section showed an almost flat RPE line. In 9 eyes, 3-D images showed a typical dome-shaped convexity within the staphyloma. OCT scans showed no outward protrusions in the external scleral surface, but marked scleral thinning was seen consistent with the 2 outward concavities of the RPE. The sclera of the fovea (518.6 ± 97.6 μm) was significantly thicker than that in all 4 quadrants of the parafoveal area (range, 277.2 to 360.3 μm; $P < .001$).

• CONCLUSIONS: In highly myopic eyes with a dome-shaped macula, a horizontal ridge is formed within the posterior staphyloma by uneven thinning of the sclera. (Am J Ophthalmol 2013;155:320–328.

AJO.com Supplemental Material available at AJO.com
Accepted for publication Aug 21, 2012.

From the Department of Ophthalmology and Visual Sciences, Kyoto University Graduate School of Medicine, Kyoto, Japan (A.A.E., A.T., A.M., K.Y., A.O., S.O., I.N., Y.A.-K., M.M., N.Y.); the Department of Ophthalmology, Suez Canal University, Faculty of Medicine, Ismailia, Egypt (A.A.E., H.S.E., T.M.R., K.A.Z.); and Topcon Corporation, Tokyo, Japan (A.M.).

Inquiries to Akitaka Tsujikawa, Department of Ophthalmology and Visual Sciences, Kyoto University Graduate School of Medicine, Sakyo-ku, Kyoto 606-8507, Japan; e-mail: tujikawa@kuhp.kyoto-u.ac.jp

HIGH MYOPIA IS ONE OF THE LEADING CAUSES OF visual disturbance worldwide and is particularly prevalent in Asians.[1–3] Axial elongation of the globe leads to complex changes in the topography of the posterior pole, with concomitant thinning of the retina, choroid, and sclera and subsequent development of macular pathologic features.[4–6] Posterior staphyloma, which is one of the characteristic features of high myopia, has been reported to be associated with various vision-threatening complications, including choroidal neovascularization, macular holes, schisis, chorioretinal atrophy, and visual field defects.[4–6] Using fundus examination, Curtin classified posterior staphyloma in eyes with high myopia into 10 types.[4]

Based on optical coherence tomography (OCT), a dome-shaped macula was first described by Gaucher and associates as an unexpected finding in myopic staphyloma and was characterized as an inward convexity of the macula that occurred in highly myopic eyes within the concavity of a posterior staphyloma.[7] They suggested that the dome-shaped macula may be the result of changes in choroidal thickness or to changes in scleral shape in highly myopic eyes. Subsequently, Imamura and associates, by using enhanced depth imaging OCT, reported that the dome-shaped macula is the result of a localized variation in thickness of the sclera in the macular area.[8,9] However, the mechanisms that underlie this unusual tomographic feature remain unknown. In addition, most cases of dome-shaped macula in these previous reports were examined by only unidirectional OCT scans.[7,8,10,11] So far, little information is available on the topography of the posterior pole in eyes with a dome-shaped macula.

With the advances in OCT in the last decade, several retinal pathologic characteristics have been identified in highly myopic eyes.[12–19] However, imaging of highly myopic eyes with conventional OCT systems has several difficulties. Recent OCT generation has used swept-source laser as a light source.[20–27] The swept-source OCT at a longer wavelength allows deeper tissue penetration into the choroid and even sclera, especially in highly myopic eyes. Additionally, the higher imaging speed, larger scan window, and lower sensitivity roll-off with depth allow for larger scans and the production of 3-dimensional (3-D)

0002-9394/09/$36.00
http://dx.doi.org/10.1016/j.ajo.2012.08.007

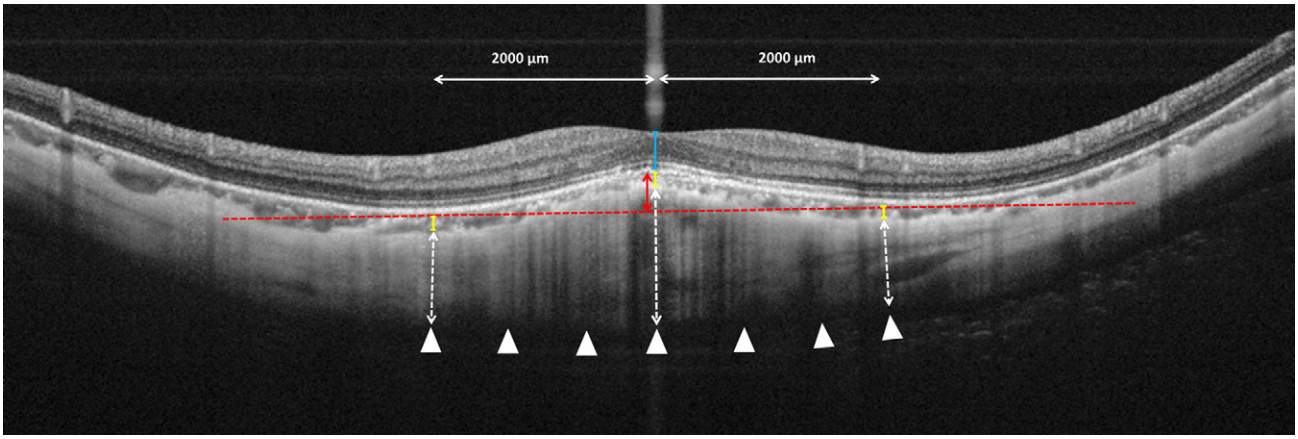

FIGURE 1. Parameters associated with the dome-shaped macular configuration as measured from a multiaveraged vertical section obtained with swept-source optical coherence tomography. At the fovea, 3 parameters were measured: retinal thickness (blue line), choroidal thickness (yellow line), and scleral thickness (dashed white double arrow). The height of the inward bulge of the retinal pigment epithelium (red double arrow) was measured above the tangent plane (red dashed line) at the bottom of the posterior pole. At points 2000 µm superior and 2000 µm inferior to the fovea, the choroidal (yellow line) and scleral (dashed white double arrow) thicknesses were measured. In the horizontal scan, choroidal and scleral thicknesses also were measured at 2000 µm temporal and nasal to the fovea. White arrowheads indicate the outer scleral border.

images of the posterior pole. In the study described herein, we examined eyes with a dome-shaped macula using swept-source OCT at a longer wavelength to study the pathomorphologic features of the dome-shaped macula by 3-D imaging and to elucidate its association with macular complications.

METHODS

THE INSTITUTIONAL REVIEW BOARD AND ETHICS Committee of Kyoto University approved this prospective study, which adhered to the tenets of the Declaration of Helsinki. Written informed consent for research participation was obtained from each subject before examination.

In the current prospective cross-sectional study, we examined 51 eyes (35 patients) with high myopia who demonstrated a dome-shaped macular configuration within the posterior staphyloma. The macular area of the study subjects was examined using a prototype swept-source OCT at Kyoto University Hospital between the beginning of September 2010 and the end of February 2012. The diagnosis of a dome-shaped macula was based on the OCT findings of an inward bulge inside the chorioretinal posterior concavity of the macular area, according to the description of Gaucher and associates.[7] This unusual feature of the macula in eyes with a dome-shaped macula is especially clear on the vertical scans,[7] and performing long vertical scans has been recommended to discern specific features.[28] In the current study, we recruited patients with highly myopic eyes with a dome-shaped macula on the basis of the presence of an inward bulge of the retinal pigment epithelium (RPE) of more than 50 µm on vertical sections of OCT (Figure 1) above a presumed line tangent to the outer surface of RPE at the bottom of the posterior staphyloma. High myopia was defined as a refractive error of −6.0 diopters or more, an axial length of 26.5 mm or more, or both. Eyes were excluded if they had a pre-existing ocular disease or if they had a history of ocular surgery, other than cataract surgery. The original refractive errors were used for eyes that underwent cataract surgery. The type of posterior staphyloma was determined by location and size according to the classification of Curtin.[4] In the current study, eyes with an inferior posterior staphyloma (type V) were excluded. All eyes of our patients had a posterior staphyloma of type I, II, III, or IX.

All subjects underwent a comprehensive ocular examination, including autorefractometry (ARK1; Nidek, Gamagori, Japan), best-corrected visual acuity measurement with a 5-m Landolt chart, axial length measurement using ocular biometry (IOLMaster; Carl Zeiss Meditec, Jena, Germany), slit-lamp examination, intraocular pressure measurement, dilated color fundus photography (TRC50LX; Topcon Corp, Tokyo, Japan), and swept-source OCT examination. All eyes with macular complications underwent simultaneous fluorescein angiography and indocyanine green angiography using Spectralis HRA+OCT (Heidelberg Engineering, Heidelberg, Germany). Eyes with poor images resulting from opaque media (eg, cataracts or corneal opacity) were excluded from the study.

• **SWEPT-SOURCE OPTICAL COHERENCE TOMOGRAPHY AND SCAN PROTOCOLS:** The prototype swept-source OCT (Topcon Corp) used in the current study has been described previously.[20,21] In brief, this swept-source OCT

uses a light source of a wavelength-sweeping laser centered at 1050 nm, with a repetition rate of 100 000 Hz. This OCT system has a depth of 2.6 mm in the scan window. Swept-source OCT examinations of the eligible subjects were performed by trained examiners (A.A.E., A.M.) after pupil dilation.

In each subject, multiaveraged horizontal and vertical raster scans of 12 mm were obtained. Fifty single images, where each image consisted of 1024 A-scans, were registered and averaged by software to create a multiaveraged single image. The vertical scan was centered on the fovea, whereas the horizontal scan was centered on the midpoint between the fovea and optic disc.

3-D imaging data sets were acquired by using a raster scan protocol of 512 (horizontal) × 128 (vertical) A-scans per data set in 0.8 seconds. Each raster scan consisted of 128 B-scans and covered an area of 12 × 8 mm^2 centered on the fovea. Centration was confirmed by internal fixation and by a built-in camera within the swept-source OCT system. To improve the signal-to-noise ratio, each image was despeckled by the weighted moving averaging of three consecutive original B-scans. In each image, the RPE line was determined using the built-in automated segmentation-modifying tool, with manual corrections if necessary. 3-D images were constructed to represent the curvature of the posterior pole.

• **CHOROIDAL AND SCLERAL THICKNESS MEASUREMENT PROTOCOL:** Using the multiaveraged OCT images, we measured the choroidal and scleral thicknesses at the center of the fovea and at surrounding parafoveal regions at 2000 μm superiorly, inferiorly, temporally, and nasally, respectively. Retinal thickness was defined as the distance between the vitreoretinal interface and the outer border of the RPE; choroidal thickness was defined as the distance between the outer border of the RPE line and the chorioscleral interface; scleral thickness was defined as the distance between the chorioscleral interface and outer scleral border. Retinal, choroidal, and scleral thicknesses at the fovea were calculated as the average of the measurements in the vertical and horizontal OCT images at the fovea. We also measured the height of the inward bulge of the RPE above a presumed line tangent to the RPE at the bottom of the posterior staphyloma (Figure 1).

The outer surface of the sclera was identified carefully in the OCT scans from retro-ocular structures such as episcleral tissue, the Tenon capsule, inferior oblique aponeurosis, or orbital fat. Scleral tissues were identified by their lamellar morphologic features, continuity of the outer surface of the sclera within the 7 raster lines in the vertical and horizontal scans, and high reflectivity values. The outer border of the sclera at the fovea exceeded the scan window in 2 eyes, and the outer scleral border was not clearly visible in 3 eyes. In these 5 eyes, we used the greatest measurable scleral thickness. In the parafoveal region, the scleral thickness could be identified in all eyes.

TABLE 1. Characteristics of Eyes With a Dome-Shaped Macula

No. of eyes/patients	51/35
Sex (male/female)	8/27
Age (years)	65.6 ± 11.3 (40 to 87)
Axial length (mm)	29.53 ± 2.16 (26.16 to 34.89)
Refractive error (D)	−13.69 ± 5.86 (−6.75 to −31.0)
Visual acuity (logMAR)	0.36 ± 0.39 (−0.18 to 1.40)
Intraocular pressure (mm Hg)	14.8 ± 2.7 (9 to 22)
Height of inward bulge[a] (μm)	152.3 ± 58.8 (56.0 to 294.0)
Foveal retinal thickness (μm)	190.9 ± 84.9 (0.0 to 522.5)
Foveal choroidal thickness (μm)	34.5 ± 29.0 (10.0 to 117.5)
Foveal scleral thickness (μm)	518.6 ± 97.6 (316.0 to 711.0)
Type of posterior staphyloma	
I	18
II	26
III	3
IX	4

D = diopter; logMAR = logarithm of minimal angle of resolution.

[a]The height of the inward bulge was measured from a presumed line tangent to the outer surface of retinal pigment epithelium at the bottom of the posterior staphyloma in the vertical section of optical coherence tomography.

• **STATISTICAL ANALYSIS:** Statistical analysis was computed using SPSS statistical software version 16 (SPSS Inc, Chicago, Illinois, USA). All values are expressed as mean ± standard deviation. The measured visual acuity was converted to the logarithm of the minimal angle of resolution (logMAR) units for statistical analysis. The data were analyzed using the unpaired *t* test. The Fisher exact test was used to analyze categorical variables. Choroidal and scleral thicknesses within different regions were compared using the 1-way analysis of variance with Tukey post hoc analysis. A *P* value of less than .05 was considered to be statistically significant.

RESULTS

IN THE CURRENT STUDY, 51 EYES OF 35 PATIENTS (8 MEN AND 27 women) with a dome-shaped macula were studied by swept-source OCT at a 1-μm wavelength. The characteristics of the subjects are summarized in Table 1. Their mean age was 65.6 ± 11.3 years (range, 40 to 87 years). Mean refractive error was −13.69 ± 5.86 diopters (range, −6.75 to −31.00 diopters), and mean axial length was 29.53 ± 2.16 mm (range, 26.16 to 34.89 mm). Mean visual acuity was 0.36 ± 0.39 logMAR (range, −0.18 to 1.40 logMAR). The dome-shaped macula was bilateral in 16 (45.7%) patients, and all patients were Japanese.

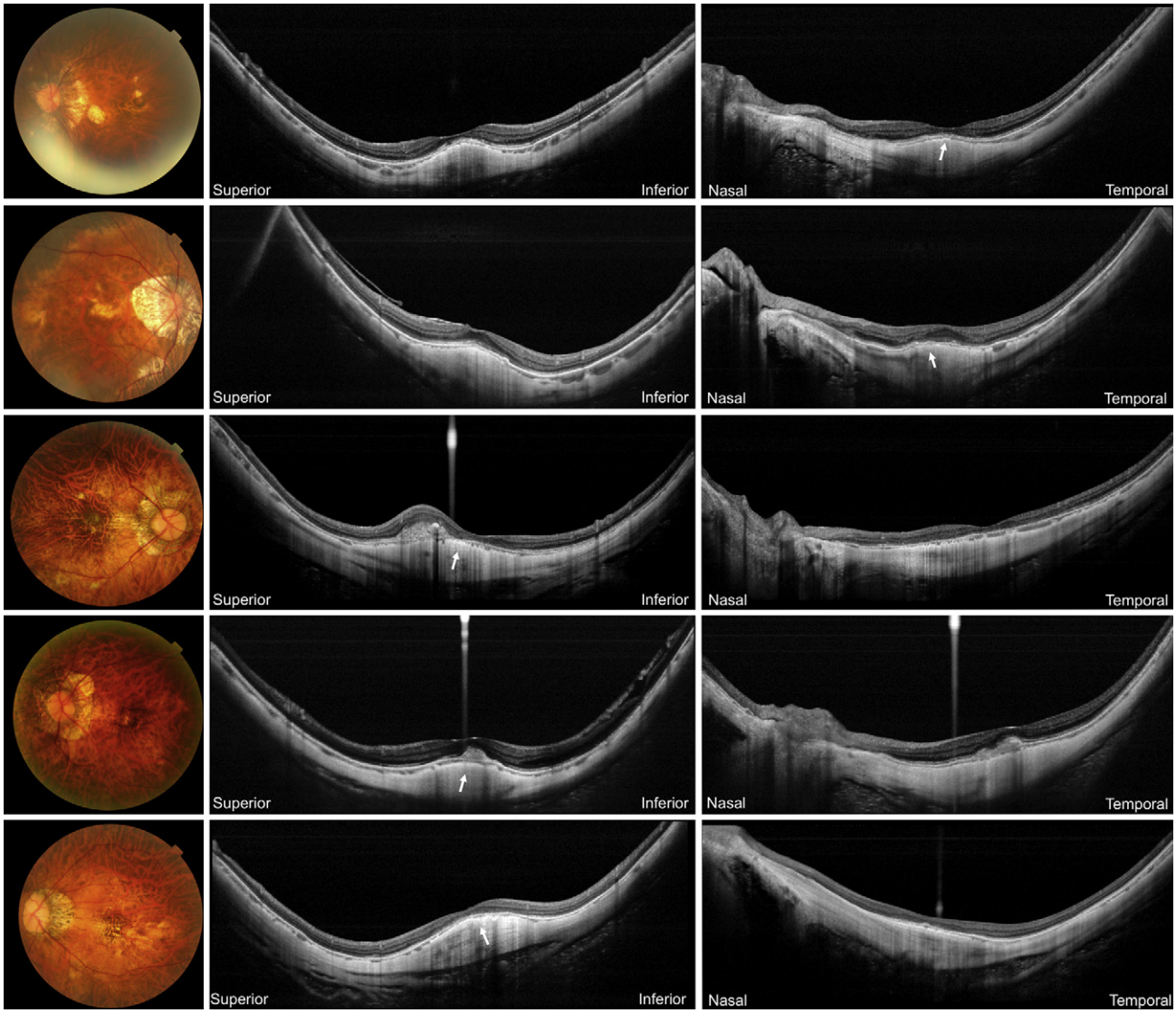

FIGURE 2. Eyes with high myopia that show dome-shaped macular configuration within the posterior staphyloma. (Left) Fundus photograph. (Middle and right) Multiaveraged vertical (middle) and horizontal (right) scans through the fovea obtained by swept-source optical coherence tomography (OCT). (Top row) Both vertical and horizontal OCT scans show an inward convexity of the retinal pigment epithelium (RPE) within the staphyloma. The inward bulge is seen more clearly in the vertical scan. The top of the bulge (arrow) is located beneath the fovea. (Second row) Both vertical and horizontal OCT scans show an inward convexity of the RPE. The top of the bulge (arrow) is located at the nasal side of the fovea. (Third through Fifth rows) Vertical OCT scans show clearly an inward bulge of RPE within the posterior staphyloma. The top of the bulge (arrows) is located beneath the fovea. The horizontal scan shows an almost flat contour of the RPE.

• **SHAPE OF INWARD PROTRUSION IN EYES WITH DOME-SHAPED MACULAS:** Multiaveraged sections with the swept-source OCT enabled clear visualization of the structure of the retina, choroid, and sclera. In all eyes, an inward bulge within the posterior staphyloma was seen clearly in the vertical sections. The height of the inward bulge above the tangent plane was 152.3 ± 58.8 μm (range, 56.0 to 294.0 μm). In the horizontal scan, however, the inward convexity often was detected less clearly. In some eyes, the horizontal scan showed a flat RPE line without any inward bulge within the staphyloma (Figure 2).

Reconstructed 3-D images revealed curvature of the RPE in the posterior pole. In all eyes, 2 outward concavities of RPE were seen within the posterior staphyloma, and a horizontal ridge was present between these 2 concavities, which was located at the fovea (Figure 3, Supplemental Video, and Supplemental Figures 1 and 2). In 42 eyes (82.4 %), the horizontal ridge was present as a band shape and the vertical scan through the fovea showed a convex configuration, but the horizontal scan showed an almost flat RPE line. In the other 9 eyes (17.6%), 3-D imaging of the

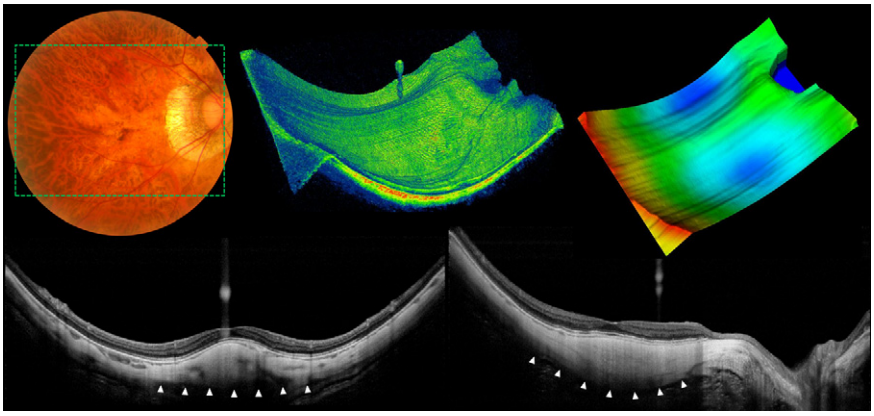

FIGURE 3. An eye with high myopia showing a band-shaped ridge within the posterior staphyloma. (Top left) Fundus photograph of the right eye of a 61-year-old woman (visual acuity, 20/20). Axial length was 28.60 mm and refractive error was −12.5 diopters. The dashed green rectangle outlines the area (12 × 8 mm^2) scanned by swept-source optical coherence tomography (OCT). (Top middle) Three-dimensional reconstructed image obtained by the swept-source OCT showing an inward convexity of the retina in the posterior pole. (Top right) Three-dimensional image reconstructed by segmentation of the retinal pigment epithelium (RPE) showing 2 outward concavities within the posterior staphyloma. A horizontal ridge is formed between these 2 outward concavities. (Bottom left) A vertical 12-mm line scan showing an inward bulge of the RPE beneath the fovea. The height of the RPE line above the tangent plane was 275 μm. The external surface of the sclera shows a rather smooth curvature (white arrowheads). The sclera shows marked thinning at the areas of the 2 concavities and seems to be relatively thick beneath the fovea. (Bottom right) A horizontal 12-mm line scan showing an almost flat contour of the RPE. The scleral thinning at the parafoveal area is less evident, compared with the areas of the 2 outward concavities within the staphyloma.

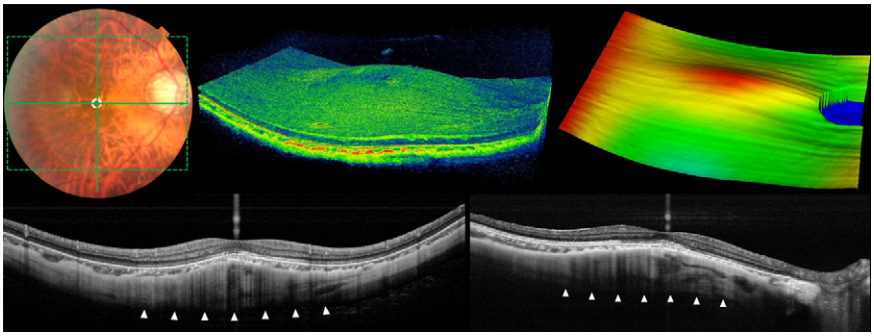

FIGURE 4. An eye with high myopia that showing a dome-shaped convexity within the posterior staphyloma. (Top left) Fundus photograph of the right eye of a 41-year-old woman (visual acuity, 20/25). Refractive error was −14.0 diopters and the axial length was 29.24 mm. The dashed green rectangle outlines the area (12 × 8 mm^2) scanned by swept-source optical coherence tomography (OCT). Vertical and horizontal multiaveraged scans of 12 mm were obtained along the green arrows. (Top middle) Three-dimensional reconstructed image obtained by swept-source OCT showing an inward convexity of the retina in the posterior pole. (Top right) Three-dimensional image reconstructed by segmentation of the retinal pigment epithelium (RPE) showing the typical dome-shaped convexity within the staphyloma. (Bottom left) Vertical 12-mm line scan clearly showing an inward bulge of the RPE beneath the fovea. The height of the bulge of the RPE line above the tangent plane is 163 μm. The external surface of the sclera is seen clearly (white arrowheads), and the sclera shows uneven thinning in the posterior pole, being relatively thick beneath the fovea. (Bottom right) A horizontal 12-mm line scan also shows an inward convexity in the posterior pole.

RPE showed a typical dome-shaped convexity within the staphyloma (Figure 4), and both vertical and horizontal OCT scans showed a convex configuration. Of these 9 (17.6%) eyes, the top of the convexity was located beneath the fovea in 7 (13.7%) eyes and was most prominent at the nasal side of the fovea in 2 (3.9%) eyes.

In 2 patients, one eye showed the typical dome-shaped convexity and the other eye showed a band-shaped ridge. There were no significant differences in axial length, refractive error, or choroidal thickness at the fovea or the height of the inward bulge between these 2 types. However, the foveal scleral thickness was significantly

TABLE 2. Choroidal and Scleral Thickness Within the Macular Area in Eyes With a Dome-Shaped Macula

	Choroidal Thickness, μm (*P* Value[a])	Scleral Thickness, μm (*P* Value,[a] *P* Value[b])
Subfovea	34.5 ± 29.0	518.6 ± 97.6 (NA, < .001)
Parafovea at 2000 μm superiorly	49.8 ± 37.8 (.065)	277.2 ± 97.1 (< .001, < .001)
Parafovea at 2000 μm inferiorly	40.1 ± 30.4 (.869)	284.9 ± 91.1 (< .001, .001)
Parafovea at 2000 μm temporally	39.0 ± 29.7 (.940)	306.0 ± 97.3 (< .001, .040)
Parafovea at 2000 μm nasally	17.8 ± 13.0 (.035)	360.3 ± 93.5 (< .001, NA)

NA = not applicable.
[a]*P* values, compared with the values in the fovea.
[b]*P* values, compared with the values in the nasal area (1-way analysis of variance with Tukey post hoc analysis).

thicker in eyes with a dome-shaped convexity (598.3 ± 76.8 μm) than in eyes with a band-shaped ridge (501.5 ± 93.6 μm; $P = .006$).

• **THICKNESS OF THE SCLERA IN DOME-SHAPED MACULAS:** Table 2 shows thickness of the choroid and of the sclera in the posterior pole. The choroid showed generalized thinning of the entire posterior pole (34.5 ± 29.0 μm in the fovea). In OCT scans, no outward protrusions were seen in the external surface of the sclera. However, the sclera in the posterior pole showed an uneven thickness consistent with the 2 outward concavities of RPE within the staphyloma. The OCT sections showed marked scleral thinning. In the fovea, the sclera was relatively thick (518.6 ± 97.6 μm) compared with parafoveal areas in all 4 quadrants (range, 277.2 to 360.3 μm; $P < .001$, respectively). In addition, the scleral thickness was reduced more markedly in the superior and inferior parafoveal areas than in the nasal or temporal parafoveal areas. The scleral thickness at 2000 μm superiorly and inferiorly was significantly less than that nasally ($P < .001$ and $P = .001$, respectively).

• **MACULAR COMPLICATIONS:** Table 3 shows the macular complications seen in our patients. Of the 51 eyes with dome-shaped macula, a full-thickness macular hole was seen in only 1 patient (1.9%). Extrafoveal retinal schisis was seen in 9 eyes (17.6%), but foveal schisis was seen in only 1 eye (1.9%). Twenty-one eyes (41.2%) showed choroidal neovascularization (CNV). Of these 21eyes, 12 had been treated with anti-vascular endothelial growth factor agents, 4 had received photodynamic therapy, and 2 had received photodynamic therapy combined with anti-vascular endothelial growth factor agents.

TABLE 3. Complications in the Eyes With a Dome-Shaped Macula

Choroidal neovascularization	21 (41.2%)
Serous retinal detachment	3 (5.9%)
Diffuse chorioretinal atrophy	15 (29.4%)
Patchy chorioretinal atrophy	4 (7.8%)
Lamellar macular hole	3 (5.9%)
Full-thickness macular hole	1 (1.9%)
Foveal schisis	1 (1.9%)
Extrafoveal retinal schisis	9 (17.6%)

Table 4 shows the comparison between eyes with CNV and eyes without CNV in the current study subjects. Visual acuity was significantly poorer in eyes with CNV (0.53 ± 0.42 logMAR) than in eyes without CNV (0.24 ± 0.32 logMAR; $P = .007$), but there were no differences in axial length, refractive error, or retinal, choroidal, or scleral thicknesses at the fovea between these 2 groups. However, the mean height of the inward bulge was significantly less in eyes with CNV (131.0 ± 51.7 μm) than in eyes without CNV (167.3 ± 59.5 μm; $P = .028$).

DISCUSSION

WITH THE USE OF A LIGHT SOURCE AT THIS LONGER WAVELENGTH, the current swept-source OCT allows high-contrast, long-penetration imaging of the entire choroid and sclera. When eyes with high myopia are scanned with a conventional OCT, the obtained images often are partially inverted or folded because of the limit of the scan window. The tunable laser source of the swept-source OCT has a lower signal decay versus depth compared with the existing spectral-domain OCT systems. Having a long scan window depth, the swept-source OCT used in the current study allows entire line scans of 12 mm, even in highly myopic eyes with posterior staphyloma. In addition, high-speed scanning coupled with the high sensitivity allowed high density scanning of the macular area (12×8 mm^2). By segmentation of the RPE line by means of the automated built-in software, we constructed 3-D images of the curvature of the posterior pole in eyes with a dome-shaped macula.

The dome-shaped macula was first described by Gaucher and associates in 2008 as an inward bulge of the macula in highly myopic eyes within the concavity of posterior staphyloma.[7] However, there is no precise definition of the dome-shaped macula. Originally, the authors reported that this unusual feature of the macular profile is especially clear on vertical scans,[7] and Coco and associates recommended performing long vertical scans to identify this

TABLE 4. Characteristics of the Eyes With Dome-Shaped Macula With or Without Choroidal Neovascularization

	Eyes Without Choroidal Neovascularization	Eyes With Choroidal Neovascularization	*P* Value
No. of eyes (%)	30 (58.8%)	21 (41.2%)	
Sex (male/female)	9/21	2/19	.098[a]
Age (years)	65.5 ± 12.4	65.8 ± 10.0	.936[b]
Axial length (mm)	29.60 ± 2.13	29.45 ± 2.24	.816[b]
Refractive error (D)	−13.61 ± 6.26	−14.06 ± 5.35	.806[b]
Visual acuity (logMAR)	0.24 ± 0.32	0.53 ± 0.42	.007[b]
Foveal retinal thickness (μm)	190.1 ± 62.0	191.9 ± 111.6	.943[b]
Foveal choroidal thickness (μm)	38.5 ± 32.8	28.8 ± 21.8	.212[b]
Foveal scleral thickness (μm)	518.0 ± 109.7	519.4 ± 79.6	.958[b]
Height of the inward bulge[c] (μm)	167.3 ± 59.5	131.0 ± 51.7	.028[b]

D = diopters; logMAR = logarithm of minimal angle of resolution.

[a]Fisher exact test.

[b]Unpaired *t* test.

[c]Height of the inward bulge was measured from the presumed line tangent to the outer surface of retinal pigment epithelium at the bottom of the posterior staphyloma on vertical optical coherence tomography scans.

feature.[28] Based on these previous reports, we used numerical data for the presence of an inward bulge of the RPE of more than 50 μm on the vertical OCT section above a presumed line tangent to the RPE at the bottom of the posterior staphyloma. On vertical scans, the height of the inward bulge ranged from 56.0 to 294.0 μm. On horizontal scans, however, the inward convexity often was detected less clearly, and only 9 eyes showed an inward bulge of more than 50 μm. A recent report by Coco and associates supports our current findings: when eyes with dome-shaped macula were examined with OCT, an inward bulge of the macula was detected on both vertical and horizontal scans in 9 eyes, but only on the vertical scan in 26 eyes.[28]

In reconstructed 3-D images of the RPE, 2 outward concavities were seen within the posterior staphyloma, and a horizontal ridge was formed between these 2 concavities in all eyes. Unexpectedly, this horizontal ridge was present in the typical dome-shaped convexity in only 9 of 51 eyes; the remaining 42 eyes showed a band-shaped ridge that extended horizontally from the optic disc through the fovea. However, statistical analysis showed no major difference between the 2 types of protrusion. In addition, 2 of our patients showed a band-shaped ridge in 1 eye and a dome shaped convexity in the other eye. A dome-shape convexity that generally is recognized as a dome-shaped macula may be a variant of the more common band-shaped ridge between a pair of outward concavities within the posterior staphyloma.

Recently, Moriyama and associates studied the topography of highly myopic eyes with high-resolution MRI.[29] Although 3-D MRI reconstructs the shape of the vitreous cavity, it does contribute to our understanding of the entire shape of eyeballs with high myopia. Those authors reported that 63.3% of eyes with high myopia had more than 1 protrusion on the vitreous cavity and that eyes with 3 protrusions showed the dome-shaped macula appearance on OCT sections. These eyes had 1 nasal protrusion and 1 temporal protrusion that was divided into 2 parts, superior and inferior, separated by the macula. Their observation supports our current finding of 2 outward concavities of the RPE within the posterior staphyloma. However, we could not confirm the presence of the nasal concavity in our patients because it was sometimes beyond the limit of our scan. In 9 eyes with a dome-shaped convexity, the top of the convexity was located under the fovea in 7 eyes and was most prominent at the nasal side of the fovea in 2 eyes. The third outward concavity on the nasal side may contribute to formation of the dome-shaped convexity on the horizontal ridge.

In our patients, no outward protrusions were seen in the external surface of the sclera, although 2 outward concavities of RPE were seen within the posterior staphyloma. Imamura and associates suggested that the dome-shaped macula is the result of relatively localized variations in the thickness of the sclera beneath the macula.[8] Consistent with their report, the foveal scleral thickness in our patients was significantly greater than that of the parafoveal regions in all 4 quadrants. In addition, OCT sections showed marked scleral thinning, consistent with 2 outward concavities within the staphyloma. In our patients, scleral thickness at the fovea (518.6 ± 97.6 μm) was in between data obtained from enucleated normal eyes (0.94 ± 0.18 mm) and OCT measurements of highly myopic eyes (281 ± 85 μm).[8,30] However, the scleral thickness within the 2 outer concavities within the staphyloma (range, 277.2 to 284.9 μm) was similar to that of highly myopic eyes.

Curtin classified posterior staphylomas in eyes with high myopia into 10 types.[4] Type I and type II staphylomas are reported to be most common in the Japanese population, with type I being seen in 23.4% and type II being seen in 52.7% of individuals with high myopia.[31] In younger patients with high myopia, posterior staphyloma is detected rarely. The development of posterior staphyloma at an older age often is accompanied by scleral thinning. In eyes with high myopia, the location of the ectatic change can vary between individuals,[4] and the posterior staphyloma has been shown not only to deepen with age, but also to change its shape over time.[31] Thus, we postulate that such asymmetric expansion of the eyeball could lead to the formation of the dome-shaped macular configuration within the staphyloma. This asymmetric expansion may be

secondary to a difference in structural strength of the sclera at the fovea because of either a regional difference in the biochemical structure of scleral lamellae or because of organization of the collagen bundles that make the central part of the sclera in eyes with a dome-shaped macula mechanically stronger than are the upper or lower regions.

Although the mechanism of myopic CNV remains controversial, several factors have been reported to pose a risk for development of CNV, such as lacquer cracks, patchy atrophy, choroidal thinning, dysfunction of choroidal circulation, and posterior staphyloma protrusion.[32–37] In the current study, CNV was present in 41.2% of eyes, and the height of the inward bulge in eyes without CNV was significantly greater than that in eyes with CNV, although the reason for this finding is uncertain. In eyes with a greater dome-shaped macula, however, the change in the foveal contour from concave to convex within the incurvation of the posterior staphyloma may ameliorate the overall protrusion of the staphyloma or may alter the mechanical damage induced by lacquer cracks, resulting in a decreased risk of CNV.

It is interesting to note that, although extrafoveal retinal schisis was present in 9 eyes, only 1 eye had foveal schisis without either foveal detachment or macular hole formation. Although, in the population of the current study, the mean spherical equivalent and axial length were relatively high, the incidence of foveoschisis was lower than in previous reports.[15,38] The bulge in eyes with a dome-shaped macula may act as a macular buckle-like mechanism, indenting the fovea similar to a macular exoplant or Ando plomb device,[39–41] and thus may prevent or alleviate tractional forces over the fovea, thereby preventing schisis or detachment.

The current study had some limitations. All measurements of choroidal and scleral thicknesses were carried out manually using a built-in caliper. In addition, all study subjects were Japanese. Because the distribution of type of posterior staphyloma in Japanese persons is different from that in white persons,[31] further studies in other ethnic groups are necessary. Furthermore, the current study is cross-sectional, so additional longitudinal studies are needed to elucidate clearly the scleral changes in the formation of a dome-shaped macular configuration in eyes with high myopia. Very recently, Coco and associates postulated the concept of macular bending, defined as a smooth macular elevation found in OCT in patients with high myopia related to either a dome-shaped macula or the border of inferior staphyloma.[28] In the current study, eyes with inferior staphyloma (type V) were excluded. Although we believe that these eyes are different from those with a typical dome-shaped macula, other authors have suggested that these may be variants.[10,28]

Gaucher and associates reported that all eyes with a dome-shaped macula have a posterior staphyloma of type I or II, and Imamura and associates suggested that a dome-shaped macula is a novel posterior anatomic characteristic of some highly myopic eyes and is not a specific subtype of posterior staphyloma.[7,8] In the current study, eyes with a dome-shaped macula had either posterior staphyloma type I, II, or, less frequently, III, or IX, whereas type V was excluded. We believe that the dome-shaped macula is not related to the type of staphyloma, but rather is related to an anatomic or structural change within the sclera and can occur in eyes with any type of staphyloma.

ALL AUTHORS HAVE COMPLETED AND SUBMITTED THE ICMJE FORM FOR DISCLOSURE OF POTENTIAL CONFLICTS OF INTEREST and the following were reported. Ms Matsumoto is an employee of the Topcon Corporation; Dr Yoshimura receives financial support from the Topcon Corporation, Nidek, and Canon and is a consultant to Nidek. Publication of this article was supported in part by Grant-in-Aid for Scientific Research no. 21592256 from the Japan Society for the Promotion of Science, Tokyo, Japan; and by the Japan National Society for the Prevention of Blindness, Tokyo, Japan. Involved in Conception and design of study (A.A.E., A.T., A.M., H.S.E., T.M.R., K.A.Z., N.Y.); Data collection (A.A.E., A.M., K.Y., A.O., S.O., I.N., Y.A.-K., M.M.); Analysis and interpretation of data (A.A.E., A.T., A.M., K.Y., A.O., S.O., I.N., Y.A.-K., M.M., H.S.E., T.M.R., K.A.Z.); Writing of article (A.A.E., A.T.); Critical revision of article (A.A.E., A.T., A.M., K.Y., A.O., S.O., I.N., Y.A.-K., M.M., H.S.E., T.M.R., K.A.Z., N.Y.); and Final approval of article (A.A.E., A.T., A.M., K.Y., A.O., S.O., I.N., Y.A.-K., M.M., H.S.E., T.M.R., K.A.Z., N.Y.).

REFERENCES

1. Iwase A, Araie M, Tomidokoro A, Yamamoto T, Shimizu H, Kitazawa Y. Prevalence and causes of low vision and blindness in a Japanese adult population: the Tajimi study. *Ophthalmology* 2006;113(8):1354–1362.
2. Xu L, Wang Y, Li Y, Cui T, Li J, Jonas JB. Causes of blindness and visual impairment in urban and rural areas in Beijing: the Beijing Eye Study. *Ophthalmology* 2006;113(7):1134–1141.
3. Sawada A, Tomidokoro A, Araie M, Iwase A, Yamamoto T. Refractive errors in an elderly Japanese population: the Tajimi study. *Ophthalmology* 2008;115(2):363–370.
4. Curtin BJ. The posterior staphyloma of pathologic myopia. *Trans Am Ophthalmol Soc* 1977;75:67–86.
5. Hayashi K, Ohno-Matsui K, Shimada N, et al. Long-term pattern of progression of myopic maculopathy: a natural history study. *Ophthalmology* 2010;117(8):1595–1611.
6. McBrien NA, Gentle A. Role of the sclera in the development and pathological complications of myopia. *Prog Retin Eye Res* 2003;22(3):307–338.
7. Gaucher D, Erginay A, Lecleire-Collet A, et al. Dome-shaped macula in eyes with myopic posterior staphyloma. *Am J Ophthalmol* 2008;145(5):909–914.
8. Imamura Y, Iida T, Maruko I, Zweifel SA, Spaide RF. Enhanced depth imaging optical coherence tomography of

the sclera in dome-shaped macula. *Am J Ophthalmol* 2011; 151(2):297–302.
9. Spaide RF, Koizumi H, Pozzoni MC. Enhanced depth imaging spectral-domain optical coherence tomography. *Am J Ophthalmol* 2008;146(4):496–500.
10. Byeon SH, Chu YK. Dome-shaped macula. *Am J Ophthalmol* 2011;151(6):1101; author reply 1101–1102.
11. Mehdizadeh M, Nowroozzadeh MH. Dome-shaped macula in eyes with myopic posterior staphyloma. *Am J Ophthalmol* 2008;146(3):478; author reply 478–479.
12. Sayanagi K, Morimoto Y, Ikuno Y, Tano Y. Spectral-domain optical coherence tomographic findings in myopic foveoschisis. *Retina* 2010;30(4):623–628.
13. Costa RA, Skaf M, Melo LA Jr, et al. Retinal assessment using optical coherence tomography. *Prog Retin Eye Res* 2006; 25(3):325–353.
14. Sayanagi K, Ikuno Y, Gomi F, Tano Y. Retinal vascular microfolds in highly myopic eyes. *Am J Ophthalmol* 2005; 139(4):658–663.
15. Takano M, Kishi S. Foveal retinoschisis and retinal detachment in severely myopic eyes with posterior staphyloma. *Am J Ophthalmol* 1999;128(4):472–476.
16. Sayanagi K, Ikuno Y, Tano Y. Tractional internal limiting membrane detachment in highly myopic eyes. *Am J Ophthalmol* 2006;142(5):850–852.
17. Shimada N, Ohno-Matsui K, Nishimuta A, et al. Detection of paravascular lamellar holes and other paravascular abnormalities by optical coherence tomography in eyes with high myopia. *Ophthalmology* 2008;115(4):708–717.
18. Fujiwara T, Imamura Y, Margolis R, Slakter JS, Spaide RF. Enhanced depth imaging optical coherence tomography of the choroid in highly myopic eyes. *Am J Ophthalmol* 2009; 148(3):445–450.
19. Forte R, Cennamo G, Pascotto F, de Crecchio G. En face optical coherence tomography of the posterior pole in high myopia. *Am J Ophthalmol* 2008;145(2):281–288.
20. Ellabban AA, Tsujikawa A, Matsumoto A, et al. Macular choroidal thickness and volume in eyes with angioid streaks measured by swept source optical coherence tomography. *Am J Ophthalmol* 2012;153(6):1133–1143.
21. Hirata M, Tsujikawa A, Matsumoto A, et al. Macular choroidal thickness and volume in normal subjects measured by swept-source optical coherence tomography. *Invest Ophthalmol Vis Sci* 2011;52(8):4971–4978.
22. Ikuno Y, Maruko I, Yasuno Y, et al. Reproducibility of retinal and choroidal thickness measurements in enhanced depth imaging and high-penetration optical coherence tomography. *Invest Ophthalmol Vis Sci* 2011;52(8):5536–5540.
23. Ohno-Matsui K, Akiba M, Moriyama M, Ishibashi T, Tokoro T, Spaide RF. Imaging retrobulbar subarachnoid space around optic nerve by swept-source optical coherence tomography in eyes with pathologic myopia. *Invest Ophthalmol Vis Sci* 2011;52(13):9644–9650.
24. Ohno-Matsui K, Akiba M, Moriyama M, et al. Acquired optic nerve and peripapillary pits in pathologic myopia. *Ophthalmology* 2012;119(8):1685–1692.
25. Jirarattanasopa P, Ooto S, Tsujikawa A, et al. Assessment of macular choroidal thickness by optical coherence tomography and angiographic changes in central serous chorioretinopathy. *Ophthalmology* 2012;119(8):1666–1678.
26. Motaghiannezam R, Schwartz DM, Fraser SE. In vivo human choroidal vascular pattern visualization using high-speed swept-source optical coherence tomography at 1060 nm. *Invest Ophthalmol Vis Sci* 2012;53(4):2337–2346.
27. Maruko I, Iida T, Sugano Y, Oyamada H, Sekiryu T. Morphologic choroidal and scleral changes at the macula in tilted disc syndrome with staphyloma using optical coherence tomography. *Invest Ophthalmol Vis Sci* 2011;52(12):8763–8768.
28. Coco RM, Sanabria MR, Alegria J. Pathology associated with optical coherence tomography macular bending due to either dome-shaped macula or inferior staphyloma in myopic patients. *Ophthalmologica* 2012;228:7–12.
29. Moriyama M, Ohno-Matsui K, Hayashi K, et al. Topographic analyses of shape of eyes with pathologic myopia by high-resolution three-dimensional magnetic resonance imaging. *Ophthalmology* 2011;118(8):1626–1637.
30. Vurgese S, Panda-Jonas S, Jonas JB. Scleral thickness in human eyes. *PLoS One* 2012;7(1):e29692.
31. Hsiang HW, Ohno-Matsui K, Shimada N, et al. Clinical characteristics of posterior staphyloma in eyes with pathologic myopia. *Am J Ophthalmol* 2008;146(1):102–110.
32. Avila MP, Weiter JJ, Jalkh AE, Trempe CL, Pruett RC, Schepens CL. Natural history of choroidal neovascularization in degenerative myopia. *Ophthalmology* 1984;91(12): 1573–1581.
33. Ikuno Y, Sayanagi K, Soga K, et al. Lacquer crack formation and choroidal neovascularization in pathologic myopia. *Retina* 2008;28(8):1124–1131.
34. Ohno-Matsui K, Yoshida T, Futagami S, et al. Patchy atrophy and lacquer cracks predispose to the development of choroidal neovascularisation in pathological myopia. *Br J Ophthalmol* 2003;87(5):570–573.
35. Ikuno Y, Jo Y, Hamasaki T, Tano Y. Ocular risk factors for choroidal neovascularization in pathologic myopia. *Invest Ophthalmol Vis Sci* 2010;51(7):3721–3725.
36. Dimitrova G, Tamaki Y, Kato S, Nagahara M. Retrobulbar circulation in myopic patients with or without myopic choroidal neovascularisation. *Br J Ophthalmol* 2002;86(7): 771–773.
37. Wakabayashi T, Ikuno Y. Choroidal filling delay in choroidal neovascularisation due to pathological myopia. *Br J Ophthalmol* 2010;94(5):611–615.
38. Baba T, Ohno-Matsui K, Futagami S, et al. Prevalence and characteristics of foveal retinal detachment without macular hole in high myopia. *Am J Ophthalmol* 2003;135(3):338–342.
39. Theodossiadis GP, Theodossiadis PG. The macular buckling procedure in the treatment of retinal detachment in highly myopic eyes with macular hole and posterior staphyloma: mean follow-up of 15 years. *Retina* 2005;25(3):285–289.
40. Mateo C, Burés-Jelstrup A, Navarro R, Corcóstegui B. Macular buckling for eyes with myopic foveoschisis secondary to posterior staphyloma. *Retina* 2012;32(6):1121–1128.
41. Tanaka T, Ando F, Usui M. Episcleral macular buckling by semirigid shaped-rod exoplant for recurrent retinal detachment with macular hole in highly myopic eyes. *Retina* 2005; 25(2):147–151.

Biosketch

Abdallah A. Ellabban, MD, graduated from the Suez Canal University (Egypt) and obtained his MD in 2003. He completed a residency program and obtained a masters degree in ophthalmology from the Suez Canal University in 2007. Dr Ellabban is now in a PhD program in the Department of Ophthalmology and Visual Sciences at Kyoto University (Japan) under the supervision of Professor Nagahisa Yoshimura.

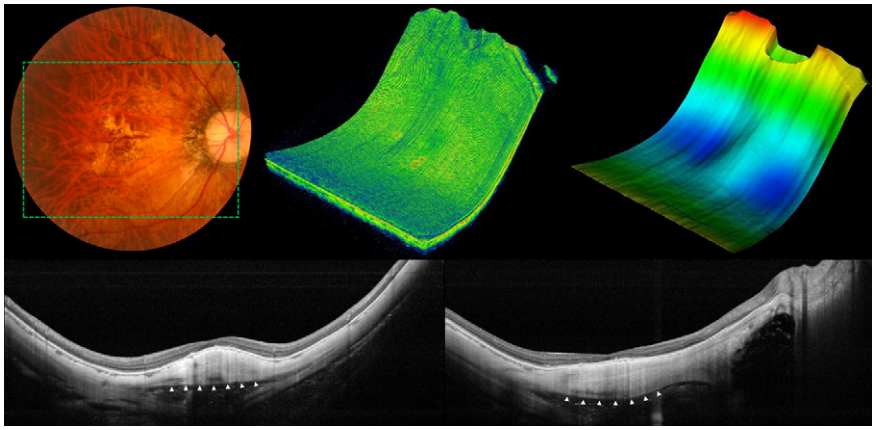

SUPPLEMENTAL FIGURE 1. An eye with high myopia showing a band-shaped ridge within the posterior staphyloma. (Top left) Fundus photograph of the right eye of a 42-year-old man (visual acuity, 20/40). Axial length was 29.19 mm and refractive error was −15.5 diopters. The dashed green rectangle outlines the area (12 × 8 mm^2) scanned by swept-source optical coherence tomography (OCT). (Top middle) Three-dimensional reconstructed image obtained by swept-source OCT showing an inward convexity of the retina at the posterior pole. (Top right) Three-dimensional image of retinal pigment epithelium (RPE) showing 2 outward concavities within the posterior staphyloma. A horizontal ridge is formed between these 2 concavities. (Bottom left) Vertical 12-mm line scan showing an inward bulge of the RPE beneath the fovea. The height of elevation of the RPE line above the tangent plane is 277 μm. The external surface of the sclera shows a rather smooth curvature (white arrowheads). The sclera shows marked thinning in the areas of the 2 concavities and seems to be relatively thick beneath the fovea. (Bottom right) Horizontal 12-mm line scan showing that the contour of the RPE is almost flat. The scleral thinning at the parafoveal area is less evident compared with the areas of the 2 outer concavities within the staphyloma.

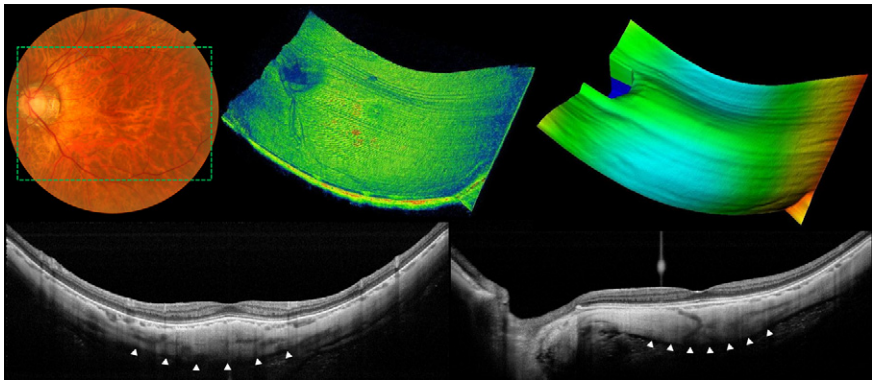

SUPPLEMENTAL FIGURE 2. An eye with high myopia showing a band-shaped ridge within the posterior staphyloma. (Top left) Fundus photograph of the right eye of a 62-year-old woman (visual acuity, 20/20). Refractive error was −12.5 diopters. The dashed green rectangle outlines the area scanned by swept-source optical coherence tomography (OCT). (Top middle) Three-dimensional reconstructed image obtained by swept-source OCT showing an inward convexity of the retina at the posterior pole. (Top right) Three-dimensional image of retinal pigment epithelium (RPE) showing 2 outward concavities within the staphyloma, with a horizontal ridge between these 2 concavities. (Bottom left) Vertical 12-mm line scan showing an inward bulge of the RPE beneath the fovea. The height of elevation of the RPE line above the tangent plane is 95 μm. The external surface of the sclera shows a rather smooth curvature (white arrowheads). The sclera shows marked thinning at the areas of the 2 concavities and seems to be relatively thick beneath the fovea. (Bottom right) Horizontal 12-mm line scan showing an almost flat contour of the RPE. The scleral thinning at the parafoveal area is less evident than within areas of the 2 outward concavities.